ANNALS OF GEOPHYSICS, 68, 5, DM574, 2025; doi:10.4401/ag-9210
OPEN ACCESS

The ANTICS Large-N Seismic Deployment in Albania

Hans Agurto-Detzel[*,1], Andreas Rietbrock[1], Frederik Tilmann[2,3], Edmond Dushi[4], Michael Frietsch[1], Ben Heit[2], Sofia-Katerina Kufner[1,5], Mike Lindner[6,7], Besian Rama[4], Bernd Schurr[2], Xiaohui Yuan[2]

(1) Karlsruhe Institute of Technology, Geophysical Institute, Germany
(2) GFZ Helmholtz Centre for Geosciences, Potsdam, Germany
(3) Freie Universität Berlin, Germany
(4) Polytechnic University of Tirana, Institute of Geosciences, Tirana, Albania
(5) Friedrich-Alexander University Erlangen-Nürnberg, GeoZentrum Nordbayern, Germany
(6) DESY, Hamburg, Germany
(7) Deutsches Zentrum für Astrophysik, Görlitz, Germany

Article history: received November 22, 2024; accepted March 27, 2025

Abstract

Located within the active continental collision between Eurasia and the Adriatic microplate, Albania is an earthquake prone country with one of the highest seismic hazard in Europe. This came into evidence when the $M_W = 6.4$ Durrës earthquake hit the country in 2019, causing 51 fatalities and widespread damage to infrastructure. Despite this stark reminder, the seismotectonics of Albania remains poorly researched, holding many unknowns regarding active seismogenic faults and 3D velocity structure. In an attempt to fill-in this knowledge gap, we conceived the project ANTICS (AlbaniaN TectonIcs of Continental Subduction) to install a temporary network of 382 seismic stations and densely monitor the abundant seismic activity in central Albania. In this paper we introduce the project goals and seismic deployment, assessing data quality and extracting valuable lessons from such a complex large-N deployment. Finally, we present some preliminary results on the detected seismicity and a receiver function profile and expand on an outlook of the project and possible next steps in the area.

Keywords: Large-N seismology; Albania; Adriatic Plate; Seismic network; Seismotectonics

1. Introduction

Albania sits in the central portion of the actively convergent boundary between the Eurasian plate and the Adriatic microplate (Fig. 1). As such, compressive tectonics with active shortening in the SW-NE direction and NW-striking thrusts and folds dominate, particularly in the coastal areas. Tectonically, the country is dominated by the presence of the Albanides, the middle section of the Dinarides-Hellenides fold-and-thrust belt that was formed east of the Adriatic Sea since the Late Jurassic as part of the large-scale convergence between Eurasia and Africa (Handy et al., 2019). The regional seismotectonics is controlled by the aforementioned system of NW-SE thrust faulting, but also by two major NE-SW strike-slip structures that control the sedimentary emplacement and tectonic

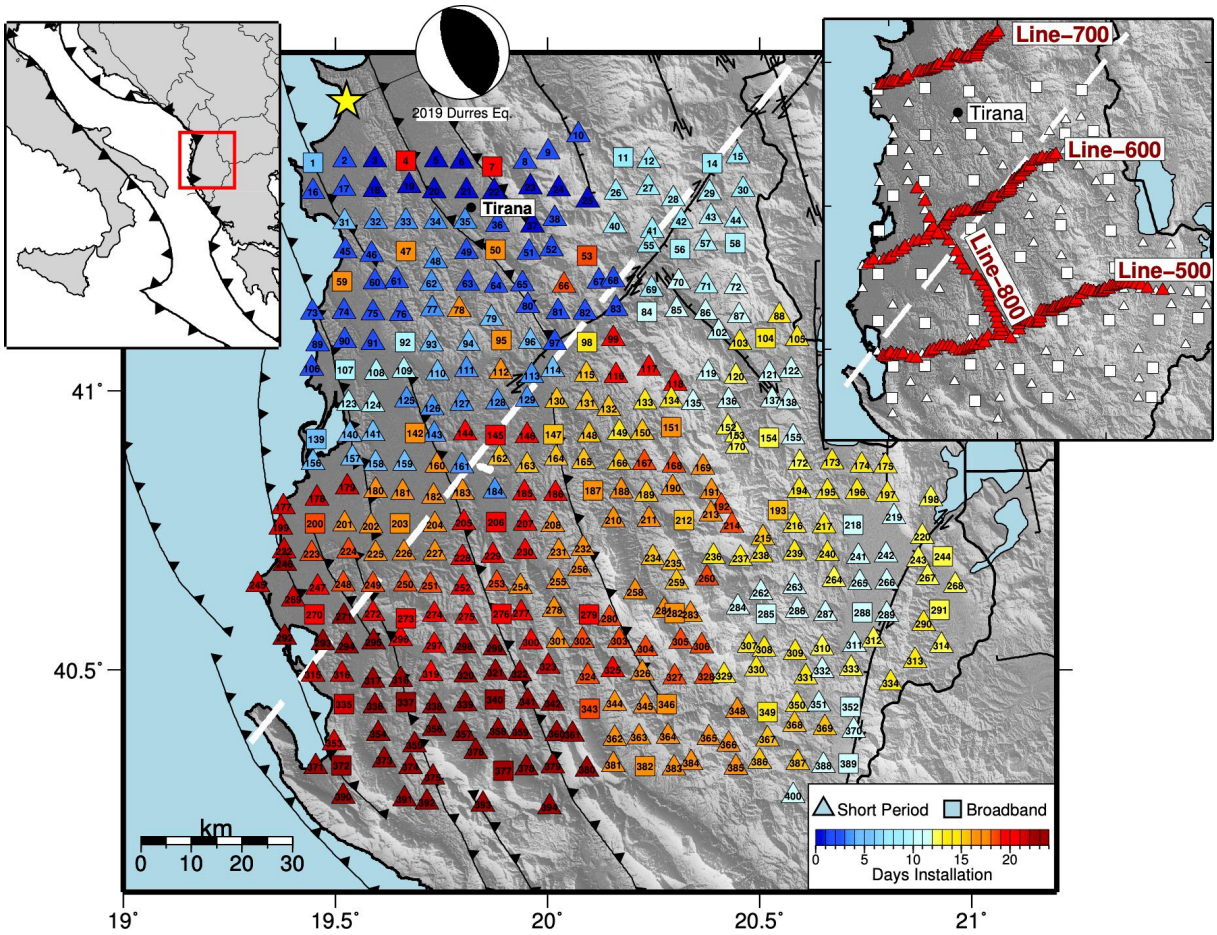

Figure 1. Location and first phase (September 2022 to May 2023) network deployment coloured by installation date. Focal mechanism of 2019 $M_w = 6.4$ Durrës earthquake (yellow star), taken from USGS moment tensor solution. Faults from Styron et al. (2020). Dashed white line shows Vlorë-Elbasan lineament. Top-right inset: receiver function lines and areal stations remaining throughout the second phase (May 2023 to April 2024).

evolution of the Albanides. These tectonic lineaments are the Shkodër-Peja Fault to the north, which separates the Albanides from the Dinarides, and the Vlorë-Elbasan lineament in the south.

The Albanides orogen is divided into two tectonic domains: (1) the Internal or Eastern Albanides, composed of metamorphic sequences, particularly Jurassic ophiolites belonging to the suture of the Tethis Ocean, and (2) the External or Western Albanides, characterized by Triassic to Eocene carbonates and Oligocene to Pliocene siliciclastic deposits. Furthermore, a large foredeep basin, the Periadriatic Depression, extends northward from the Vlorë-Elbasan lineament filled with Oligocene to Quaternary deposits. The Albanides division also reflects into the deformation style: while the External Albanides and foredeep are still undergoing shortening with active SW-verging folding and thrusting, the Internal Albanides are currently undergoing extension (Vittori et al., 2021 and references therein).

In our study region, the Moho depth increases from 25-30 km under the Adriatic Sea to 40-50 km under the Albanides axis, whilst the maximum seismogenic depth tends to follow the Moho, with hypocenters mostly in the upper crust down to 20 km depth (Grad et al., 2009; Stipcevic et al., 2020). Small earthquakes ($M < 4.5$) are ubiquitous in Albania, with an M4.5+ earthquake every 1.3 years on average (Aliaj et al., 2010; Muço et al., 2013). Most larger earthquakes ($M > 5$) occur along three well recognized seismic belts: (1) the NW-trending Ionian-Adriatic coastal thrust belt, (2) the N-S trending Peshkopia-Korçë graben fault zone at the East of the country, and (3) the transversal NE-trending Elbasani-Dibra-Tetova normal fault belt that crosses the previous two (Aliaj et al., 2004). Records of historical seismicity show 55 earthquakes with intensity (MSK) larger than VIII up until the 20th century (Aliaj et al., 2010). During the instrumental era (~1900 onwards), 418 events with $M > 4.5$ occurred up until the year 2000 (Sulstarova et al., 2001). Based on historical records, Aliaj et al. (2004) estimated the maximum earthquake magnitude for the Albanian territory to be 7.25.

Recently, in November 2019, an MW 6.4 earthquake struck the port town of Durrës with a rupture on a NNW-trending shallowly dipping thrust fault at a depth of 22 km (Papadopoulos et al., 2020; Ganas et al., 2020; Govorčin et al., 2020; Teloni et al., 2021). The complete sequence included two M > 5 foreshocks and thousands of aftershocks lasting at least throughout January 2020 (Papadopoulos et al., 2020; Van der Heiden, 2021). The occurrence of this important earthquake and the lack of studies regarding the seismogenesis and velocity structure of the Albanian territory prompted the conception of the project ANTICS (AlbaNian TectonIcs of Continental Subduction).

2. The ANTICS deployment

The large-N ANTICS deployment is an international collaborative effort by the Karlsruhe Institute of Technology (KIT, Germany), the German Research Center for Geosciences (GFZ, Germany), and the Institute of GeoSciences, Energy, Water and Environment of the Polytechnic University Tirana (PUT, Albania) that builds on our previous Durrës aftershock deployment in the region (Schurr et al., 2020). The goal of the ANTICS project is to explore in detail the seismogenic sources and velocity structure within the Albanian territory, filling in the knowledge gap persistent in this region. We aim to obtain an accurate local earthquake catalogue and a detailed crustal structure from local earthquake tomography, full waveform tomography, ambient noise tomography and receiver function analysis. The ANTICS deployment is a complementary experiment synchronous with the active phase of AdriaArray (Kolinsky et al., 2025 submitted), a backbone network of broadband stations at wider spacing, which will provide regional context to the findings. Data from AdriaArray stations within and near the footprint of ANTICS will be integrated into later analysis, but here we fully focus on the description and preliminary analysis of the ANTICS deployment. Stations from the permanent Albanian network (Dushi et al., 2025 submitted) will also be used in future analysis.

The initial network deployment (Phase 1) was carried out by five teams of two people each during a 3-week period between September 22 and October 13, 2022 (Fig. 1). All instruments were obtained from the GFZ and KIT seismic pools, with a total of 382 stations installed, including 50 broadband seismometers (Trillium Compacts with flat response up to 120 s) and 332 3-component geophones (PE-6B with 4.5 Hz corner frequency) recording at a sampling rate of 100 Hz. The average inter-station spacing was 6 km, with a total covered area of 130×145 km^2, encompassing a large part of the Albanian territory including its full W-E extension. The elevation of station sites varied from sea level to 1740 m, with an average of 533 m.

During servicing in May 2023, the network geometry was reconfigured into four profile lines for receiver function analysis (Phase 2; Fig. 1). Three lines were deployed perpendicular to the orogeny, while the fourth one was deployed along strike. The nominal inter-station spacing within the lines was 1 km, and because of terrain and logistical constraints, the installation occurred mostly along roads. A total of 214 geophone stations were moved to these new sites, while the rest of the original sites, including all 50 broadband stations, were left in place as a backbone areal distribution. A second service was carried out in September 2023 to download data and exchange batteries, with the final removal of all stations in April 2024.

The setup for each site consisted of a sensor buried at ~50 cm depth, and in a separate hole the data logger, GPS antenna, battery and cables, semi-buried and covered by an inverted plastic bucket (Fig. 2). Broadband sensors were installed over cemented concrete slabs, while geophones were simply buried in the ground using their spikes. Sensors were oriented according to magnetic north; the magnetic declination in the study region during the deployment period was +5°. DATA-CUBE 3-channel recorders were used for all stations, with a gain set at 1 for broadband sensors and 16 for short period sensors. The power source consisted of one (two for broadband stations) non-rechargeable 9v/175Ah dry alkaline battery, providing an estimated autonomy of ~9 months. Importantly, because the alkaline batteries were of type metal-air, they had to have access to fresh air and therefore we kept them in a non-waterproof setup allowing proper ventilation but potentially also allowing the access of water and insects. For stations at elevations above 1000 m where freezing temperatures were expected in winter, we opted for using sealed battery packs of lithium batteries.

The most important challenges faced during installation were related to excess of rain and flooding on the roads, unreliable GPS navigation in remote areas, and mechanical car problems mostly due to the generally poor road infrastructure. Because of the high density deployment, some of the stations (47) had to be installed outside properties in open field conditions, though all broadband sensors were installed within properties for safety reasons. During the second phase, and due to the denser and more strict location of the profiles stations, a total of 110 out of the 214 stations had to be installed outside properties.

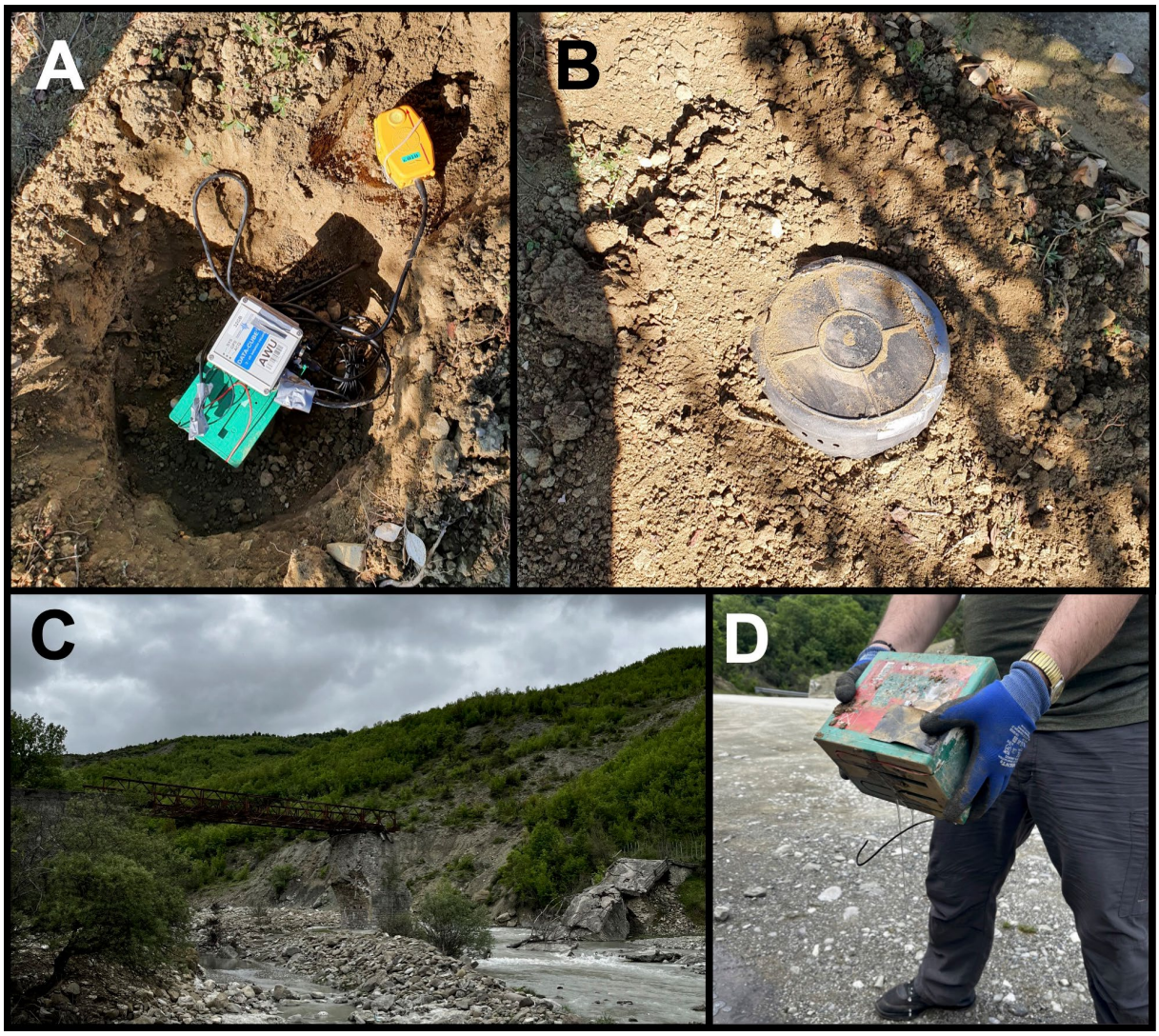

Figure 2. Composite of photos showing setup and deployment. A: initial setup with geophone, battery and Cube recorder. B: the sensor is buried and covered by soil, and the recorder and battery are covered by an inverted plastic bucket with small holes on the sides to allow for ventilation. C: Some of the difficulties during fieldwork included flooded paths and broken road infrastructure. D: flooded battery found during servicing in May 2023.

3. Data quality and recovery

Servicing of the entire network was carried out in mid-May 2023. Average data recovery for the first phase was 76% (median = 93%), with 287 (75%) stations recording for 50% of the time or more (Fig. 3). Five stations were unfortunately stolen and therefore not possible to recover.

The most common cause for incomplete data recovery was battery failure due to flooding. In fact, the average last day recorded for flooded stations was December 18, 2022, which is right after the peak of the rainy season in Albania (Fig. 4). In contrast, the average last recorded day for all stations is March 20, 2023. In total 43 (11%) sites were found with clear signs of flooding, although this is a lower bound given that flooding signs were not always visible or this information was not always collected. Notably, all the flooded sites, except for one, were installed inside a farm or backyard, mostly in clay-rich soils for a lack of a better location. Furthermore, while the average elevation for all stations was 533 m, the average elevation for flooded stations was only 294 m, which again indicates that farming soils at lower elevations had a tendency to flooding, while at higher elevations, rocky soils with better permeability were better suited for our installation. Furthermore, no battery problems were observed due to low temperatures at high altitude. Overall, during the first phase the data suggest that once a given station survived the rainy period, chances are that it recorded until the first servicing in May 2023 or shortly before that.

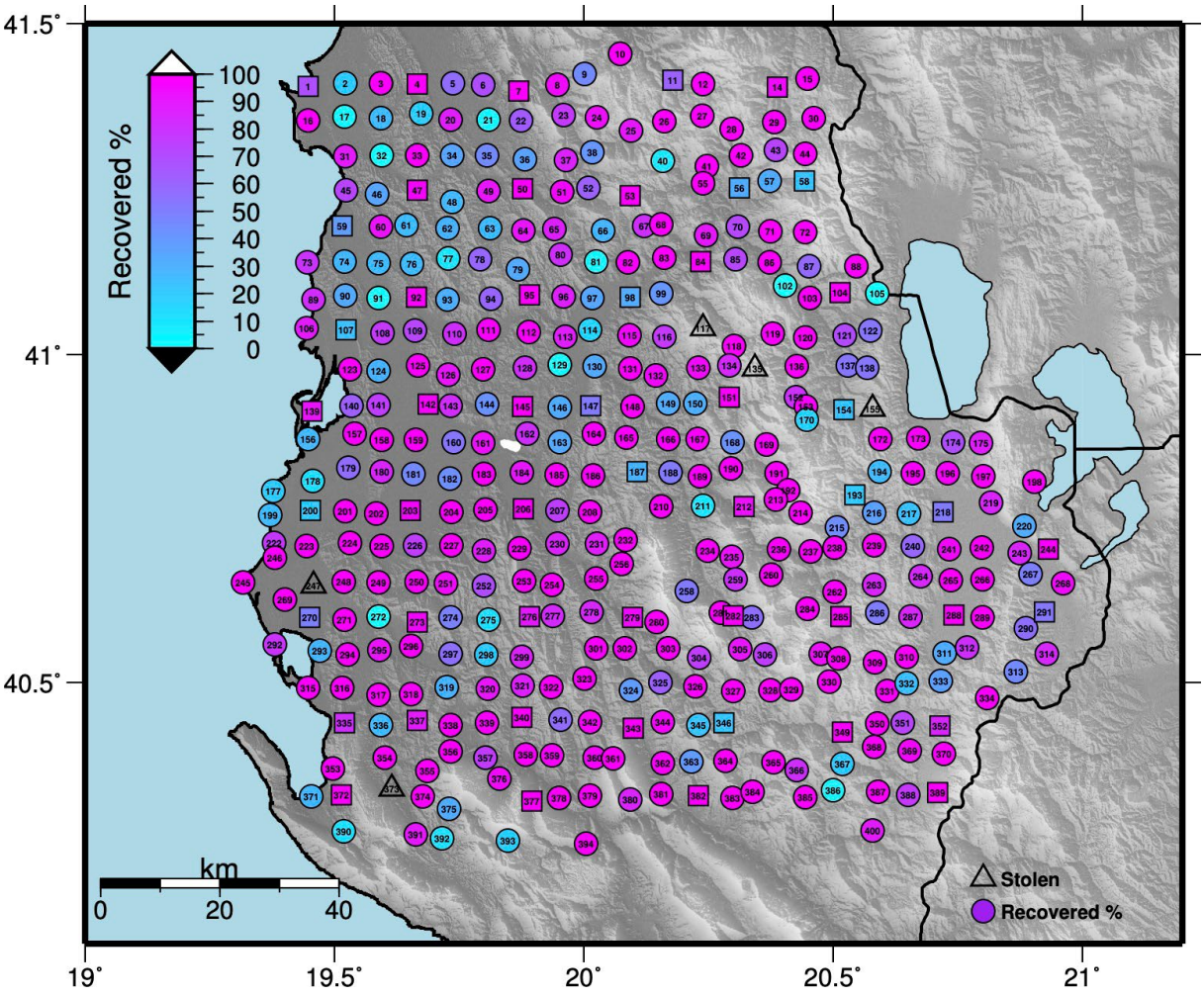

Figure 3. Data recovery during first service, May 2023.

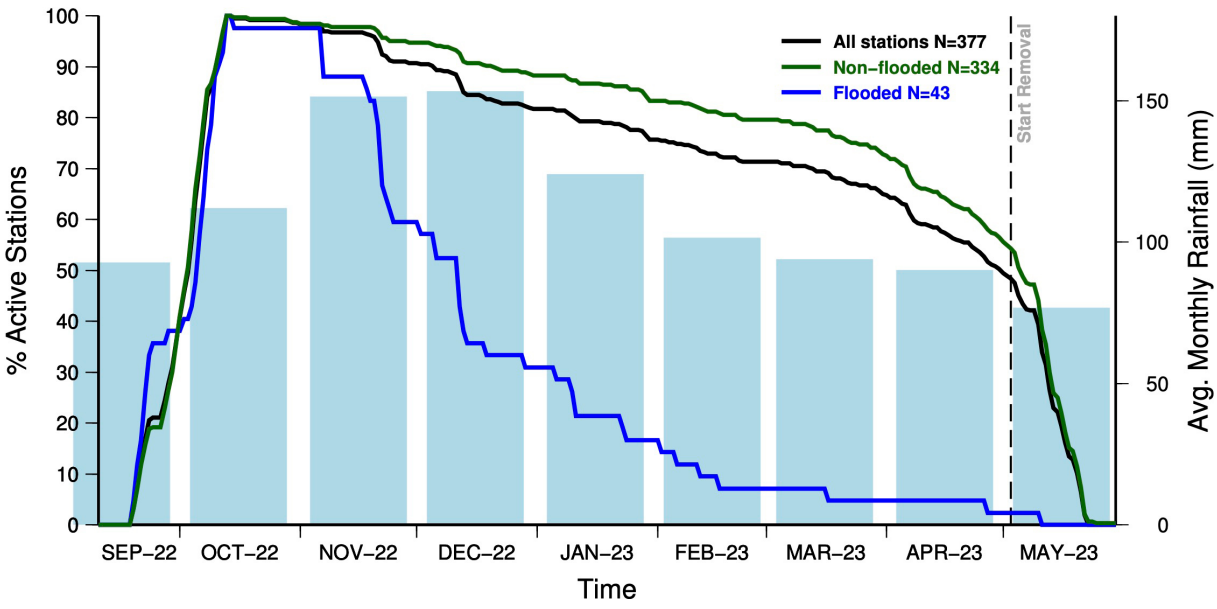

Figure 4. Correlation between active stations and historical rainfall as a function of time. A steep fall in active stations coincides with periods of heavy rainfall and therefore potential site flooding. Precipitation data from https://climateknowledgeportal.worldbank.org/country/albania/climate-data-historical (last visited 12 October 2024).

On the other hand, many of the batteries exchanged during the second service in September 2023 run out prematurely, resulting in many stations stopping acquisition in December 2023, showing no clear correlation with site conditions. We suspect that this problem was due to a bad batch of batteries with reduced capacity, although they were freshly ordered before servicing and did not show any anomalies in pre-deployment voltage checks.

Figure 5 shows the noise levels for all broadband and short-period stations during the first phase (September 2022 to May 2023) as Probabilistic Power Spectral Density (PPSD) median curves of their vertical

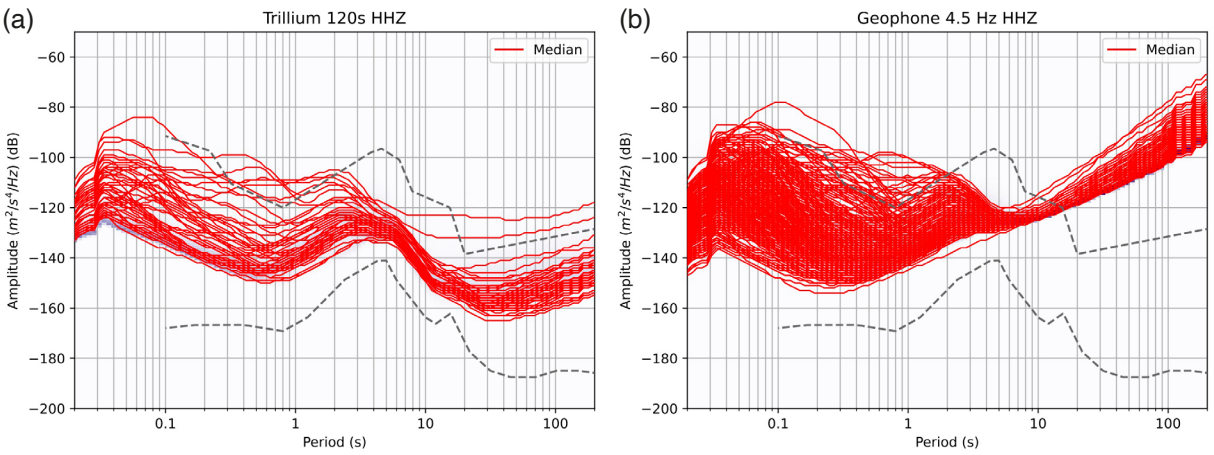

Figure 5. PPSD curves of vertical acceleration noise median for broadband (a) and short period (b) stations, corresponding to the first phase of the project (September 2022 – May 2023).

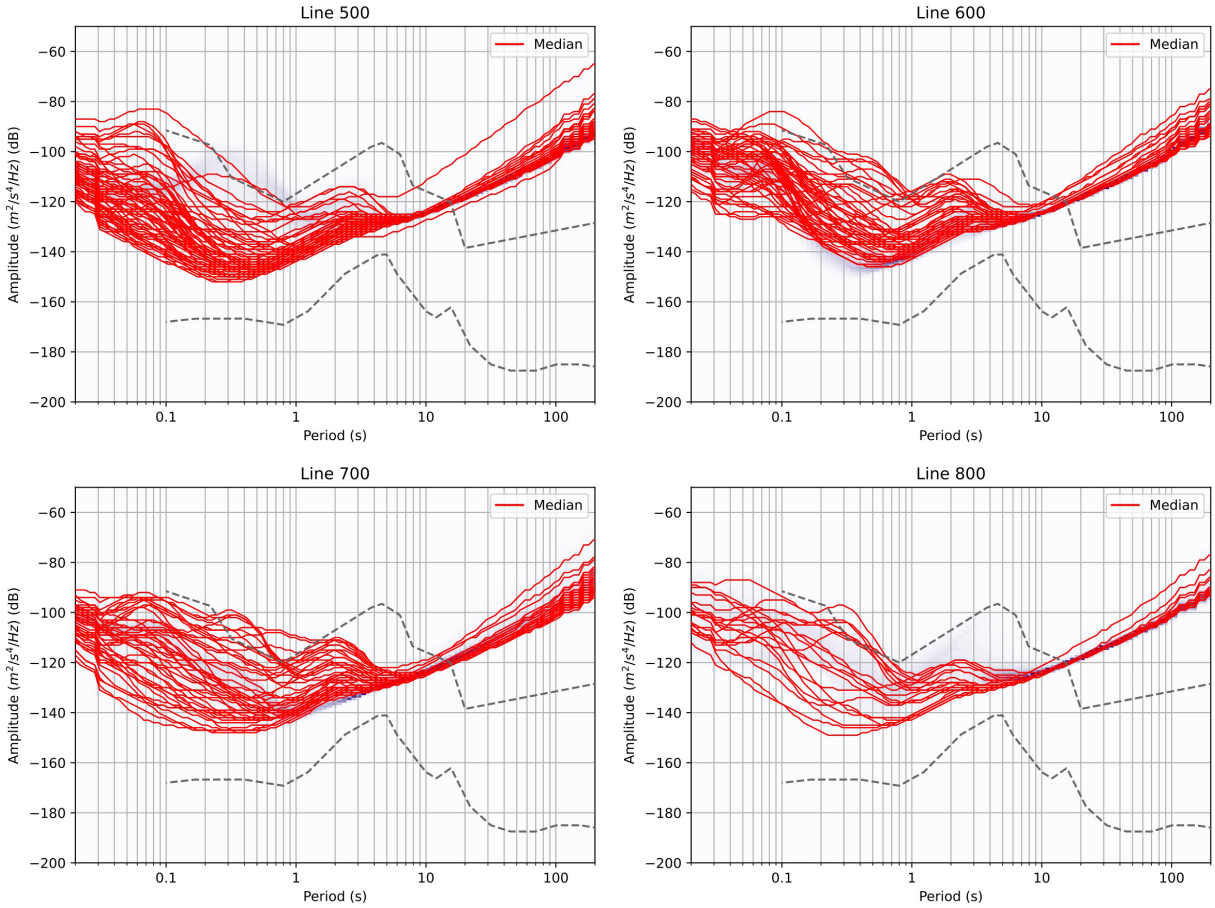

Figure 6. PPSD curves of vertical acceleration noise median for short period stations in receiver function lines, corresponding to the second phase of the project (May 2023 to April 2024).

component (e.g. Custodio et al., 2014). In general, broadband stations noise levels are below the high noise model, except for five stations that show higher noise levels at periods between 0.2 and 2 s. Geophones show a similar distribution, with higher noise levels between 0.2-2 s, and instrumental self-noise dominating for periods longer than about 5 s. The secondary microseismic noise peak occurs at 2-3 s, at significantly shorter period than the global average. In general, stations installed outside properties are considerably quieter than stations inside properties (Fig. S1), but a few free-field stations installed outside properties still present high levels of noise.

Similarly, Fig. 6 shows PPSD noise median curves for the short-period stations included in the four receiver function lines during the second phase (May 2023 to April 2024). In general, line-500 seems to be the quietest one, with the other three lines showing a more diverse range of noise amplitudes, some of them above the high noise model. Notably, line-500 was deployed in the more remote and mountainous southern area, while the other 3 lines, particularly lines 600 and 800, were deployed along important roads with nearby populated centres. This can be better seen in Fig. 7, which shows in map view the average median noise amplitude for all stations in the period band 0.05 to 2 seconds. There appears to be a clear trend from northwestern 'noisier' stations to southeastern 'quieter' stations. This can be explained as the NW contains sedimentary basins in low elevation lands close to the sea, with nearby important populated centres. On the other hand, as we move to the SE we gain in elevation, depart from the sea and the population is more scarcely distributed. A clear exemption to this rule are the noisier stations located nearby Korçë, which can be justified precisely by the presence of this city, the largest in eastern Albania, and the emplacement of Quaternary deposits in the valley. On a closer examination, a more direct first

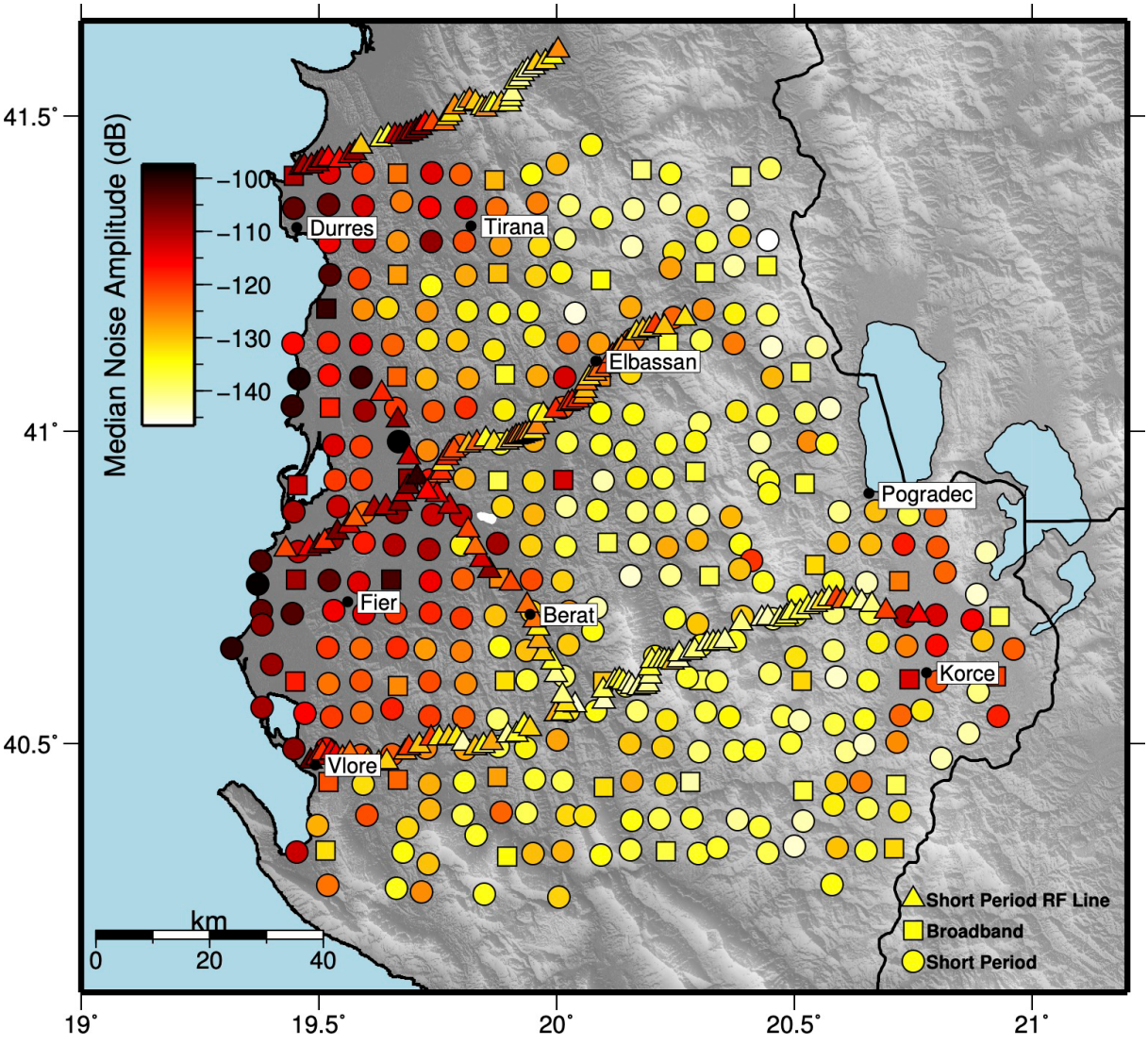

Figure 7. Average of median vertical acceleration noise amplitude per station for frequency range 0.05 to 2 s (0.5-20 Hz). Important cities indicated by black dots.

order anti-correlation seems to exist between noise amplitude and terrain slope. For example, the middle section of line-700 contains anomalously noisier stations in a flatter valley area in comparison with the surrounding stations in areas of greater slope. This also holds true for the noisier stations north of Korçë. Certainly, flatter areas are more populated and bisected by more transited roads as opposite to rough terrain where more scarce population is expected and therefore lower anthropogenic noise levels. Also, flatter areas are generally covered by a thicker sedimentary layer that amplifies the seismic noise, whilst rougher terrain often correlates with the outcrop of bed rock. In fact, the distribution of noisier stations (orange and red colours) matches well that of the Neogene-Quaternary deposits (e.g. Teloni et al., 2021). Still, it could be interesting for future deployments to consider an easily available parameter such as elevation or terrain slope as a first order indication of expected noise level (Fig. S4), in addition to other more obvious but harder to obtain parameters such as population density, road traffic or geology (e.g. Wald and Allen, 2007).

4. Preliminary Earthquake Catalogue

The continuous waveforms collected from September 2022 to May 2023 were processed with an AI-based automatic picker PhaseNet (Zhu et al., 2019), obtaining 38.4 M picks of which 20.8 M are P phases and 16.6 M are S phases. These picks were then associated into events using the AI-based HEX algorithm (Woollam et al., 2020, 2022). For this step we used a selection of 95 homogenously distributed stations given that the use of all 382 densely placed stations produced an excess of false detections. Nearly 18k events were detected with at least 8 P- and 3 S-phases, associating 1.93 M picks. All 18k events were then relocated using a 1-D velocity model (Dushi and Havskov, 2023) and the NonLinLoc algorithm (Lomax, 2009) which provides a full probabilistic density function for each hypocentral location.

Local magnitudes were calculated using maximum peak-to-peak amplitudes of the S-phase on the horizontal components and an empirical relationship for the region (Muço and Minga, 1991). We then benchmarked and corrected our estimations with 1028 common events from the manually picked local earthquake catalogue of the IGEO-PUT (Bulletin of the Albanian Seismic Network), obtaining a simple linear trend with a slope of nearly 1 but a positive bias of 0.4 magnitude units with respect to the local catalogue (Fig. 8). After correcting for this bias, our final magnitudes range from −1.0 to 4.5, with a magnitude of completeness (Mc) of ~1.5. Five earthquakes $M_L \geq 4.0$ occurred during the deployment period, the largest of them associated to the January 2023 Klos sequence.

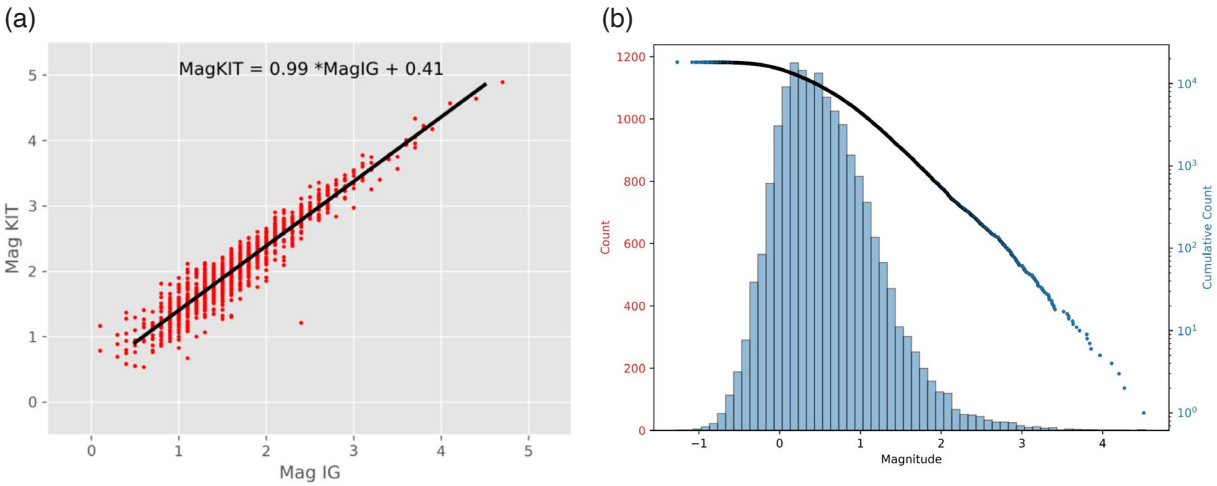

Figure 8. (a) Linear relationship between initial magnitudes from this work and from the IG-PUT local catalogue. (b) Frequency-magnitude distribution of final magnitudes.

The temporal evolution of seismicity (Fig. 9) shows an average daily rate of 70 earthquakes per day, while two maxima of 700-800 events per day are observed associated to the Klos and Erseke sequences, respectively. Figure 10 shows a selection of ~10800 events with at least 10 P, 4 S phases, and location uncertainties less than

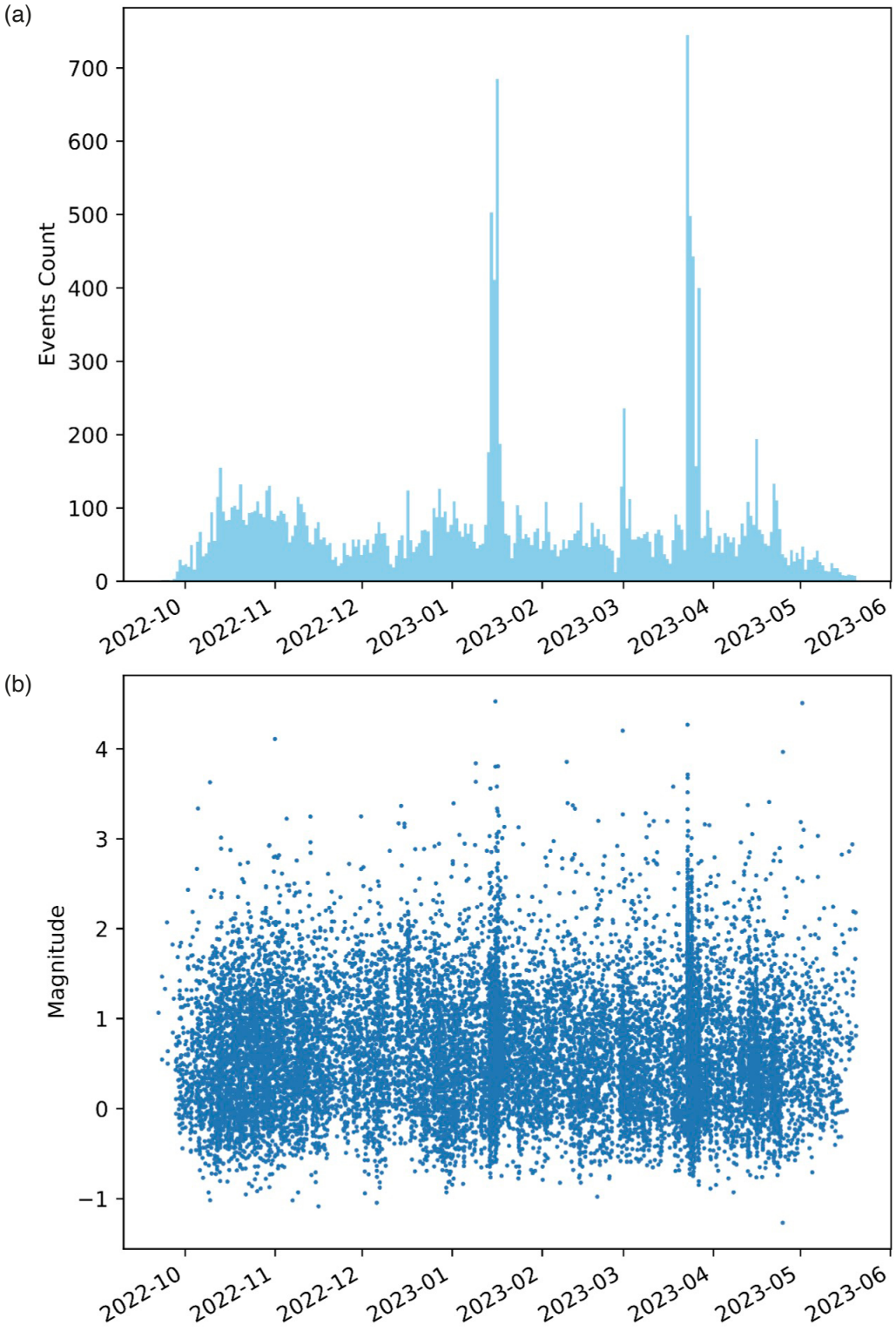

Figure 9. Temporal evolution of seismicity as daily rate (a) and magnitude occurrence (b).

5 km. The seismicity seems to be distributed in clusters and along known major structures. Events occur down to 30 km depth, notably with a decrease of the seismogenic depth from 30 to 20 km depth from North to South. Noteworthy is the fact that no seismicity is observed in the epicentral area of the 2019 Durrës earthquake, which would indicate a complete return to background seismicity levels following the aftershock period of that earthquake (Van der Heiden, 2021).

Two earthquake clusters were particularly productive during our study period: to the north, the Klos sequence occurred in January 2023, and to the south, the Erseke sequence, occurred in March 2023. The Klos sequence seems

to start in January 13 with an M_L 3.0 earthquake, which elevated the daily rate of seismicity to nearly 400 events per day in the nearby area (Fig. S6). The following next two days the seismicity rate decayed until the evening of January 15 when the M_L 4.5 mainshock occurred, which again elevated the daily rate of seismicity to above 700 events per day. The whole sequence is confined to depths 5-20 km depth, with all hypocenters $M_L \geq 3.0$ near the bottom of the seismogenic layer, ranging 15-20 km depth. Spatially, the seismicity seems to be associated to a large normal fault NW-striking. This is corroborated by our moment tensor solution (e.g. Lindner, 2023) for the Klos mainshock, which indicates oblique normal faulting with a similar strike (Fig. 10).

The Erseke sequence started with an M_L 4.3 mainshock on the 23 of March 2023, which elevated the daily rate of seismicity to almost 800 events per day in the nearby area (Fig. S7). For the next ten days, the seismicity rate decays, although some bursts of seismicity are seen on March 24 and 26 as secondary aftershock sequences of large aftershocks. The seismicity occurs mostly between 3 to 17 km depth, with the mainshock hypocenter located at 17 km. Spatially, the sequence is associated to a large oblique normal fault striking NNE (Fig. 10).

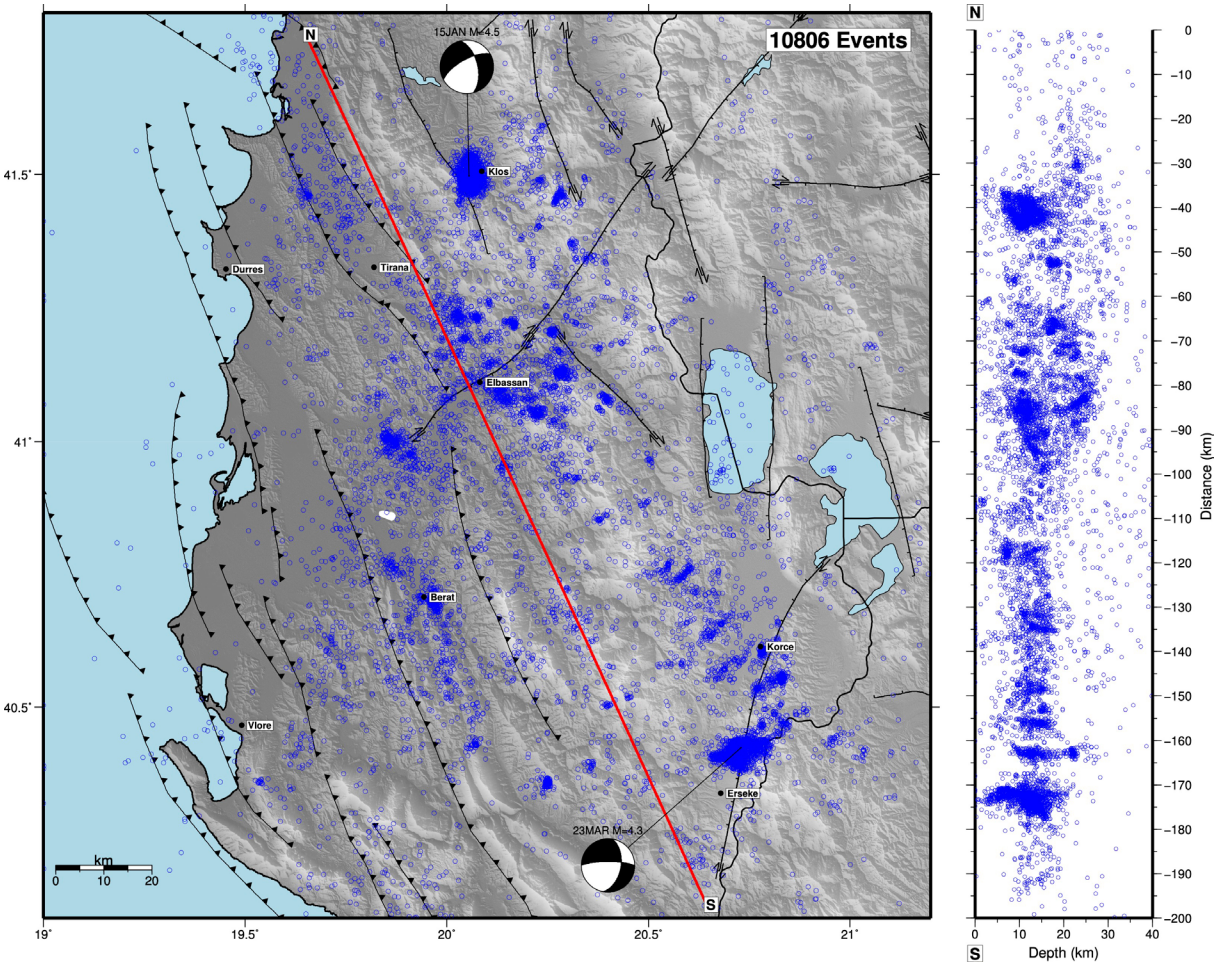

Figure 10. Seismicity map and NW-SE depth section.

5. Preliminary receiver function analysis

Passive-source seismic imaging using the receiver function (RF) method is commonly used to study the structure in the crust and upper mantle. Conventional RFs are computed using broadband data and are usually stacked over a large number of teleseismic events to enhance the signal/noise ratio. In recent years the use of short-period stations has been greatly increased and has proven successful in extracting RFs (Yuan et al., 1997; Ward et al., 2017). Here we show that it is feasible to apply the RF analysis to the ANTICS large-N experiment.

Figure 11 is a preliminary Common-Conversion-Point (CCP) stacked RF cross section along one of the linear profiles with densely spaced stations (Line-600). Ten events with magnitudes greater than 6.5 occurring between October 2022 and July 2023 are used, five in the first phase and five in the second phase of the experiment (Fig. 11a). The majority of stations are short-period geophones with a natural frequency of 4.5 Hz, which is outside the normal teleseismic frequency range usually of 0.1-1 Hz. Therefore, the instrument response has been deconvolved from the raw data to enhance teleseismic signals, as shown by Yuan et al. (1997) and Ward et al. (2017). Whereas electronic noise dominates restituted geophone records at longer periods, large teleseismic events have signals strong enough to be usable down to ~0.1 Hz. Three-component data are visually inspected and processed with the RF analysis, involving component rotation and deconvolution. RF cross sections were constructed along the four linear profiles with a swath width of 20 km. Figure 11c is an example of Line-600, along with some conspicuous crustal interfaces. The profile crosses a prominent sedimentary basin to the west and a mountainous area to the east. The interface at shallow depths down to 20 km may represent the base of the thick sediments that dips to the west (Handy et al., 2019; Rosetti et al., 2024). We note that indicated depths are biased downward as we did not correct for slower seismic velocities in the sedimentary layer in this preliminary processing. The multiples of the basement may dominate the 40-60 km depth range. There appears to be evidence of the Adriatic Moho that dips to the east to a depth of 65 km. Further analysis with the complete dataset is needed to verify these preliminary observations.

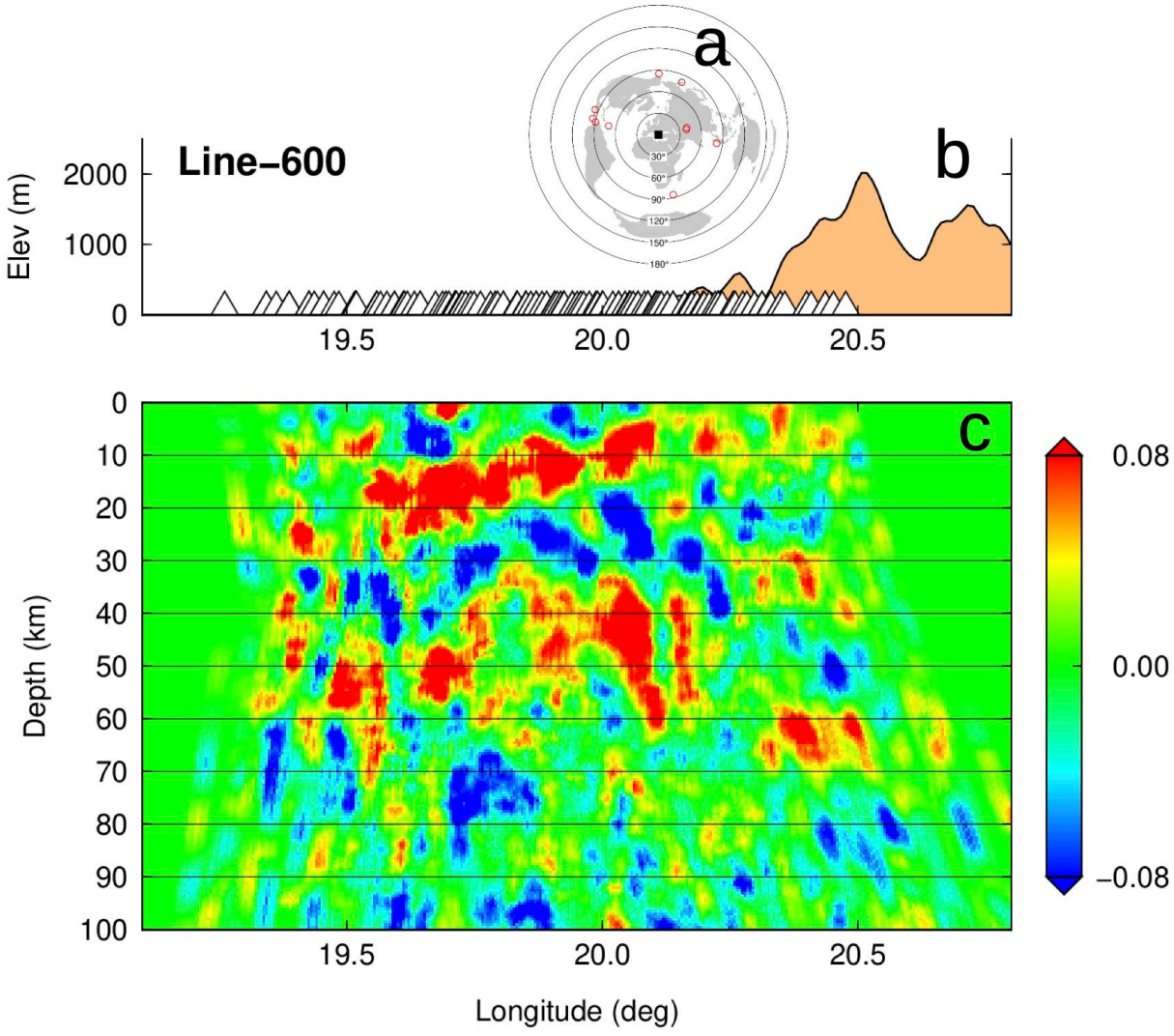

Figure 11. (a) Distribution of used teleseismic events (10); (b) Elevation profile and stations along Line-600; (c) Preliminary RF cross section showing some prominent crustal converters. Red/blue colors indicate positive/negative converted phases, representing downward velocity increase/decrease.

6. Lessons learned and outlook

Given the density and large number of installed stations, and despite the adverse road and meteorological conditions, the ANTICS deployment was swiftly and successfully achieved. In a period of three weeks during September-October 2022, we managed to install 382 seismic stations in a wide range of terrain and elevation conditions. Considering the installation and subsequent servicing, we gathered the following valuable lessons:

a) Meteorological and seasonal conditions should be taken into account for the deployment schedule to reduce the likelihood of data loss due to intense rain periods. In that sense, when a rainy period lies within the deployment period, a service run checking on the stations should be organised as soon as possible thereafter.
b) It is important to consider soil permeability of the sites, in order to avoid flooding due to poor permeability. A good rule of thumb is to avoid clay-rich soils.
c) Metal-air batteries are a good option for temporary deployments such as ours, but attention should be put into not burying too much the batteries and always keeping the upper half of it above surface to avoid penetration and accumulation of water. This of course has to be balanced with the fact that the equipment should be concealed to avoid robbery and damage when installing outside properties.
d) Once a station continued working during the rainy season, chance is that it will record until the end. In that sense, there were no problems inherent to battery durability, at least during the first phase of our experiment.
e) Having said that, battery problems did occur after the second service likely due to a bad batch of batteries with reduced capacity. Therefore, randomly checking batteries capacity before installation and, if possible, re-visiting a subset of sites after servicing is recommended in order to detect probable systematic power problems early on.

Data availability statement. The ANTICS dataset will be openly available at the GEOFON web service from May 2028 (doi:10.35097/d7zbw6eudy728tp3).

Acknowledgements. We thank the Geophysical Instrument Pool Potsdam (GIPP) for loaning the seismic equipment (loan 202214). We also acknowledge the support and funding from Karlsruhe Institute of Technology. We are indebted to all the Albanian landowners that allowed us to install stations in their properties and looked after them during the project. We also thank all the personnel involved in the installation and servicing of stations, and related logistics: Felix Bögelspacher, Kleo Allka, Rrezart Bozo, Benedikt Braszus, Gazmir Çela, Arnaud Dalsuc, Marson Dyrmishi, Almir Gjata, Altin Gjonaj, Olgert Gjuzi, Hamdi Hasa, Susanne Hemmleb, Rune Helk, Laura Hillmann, Damiano Koxhaj, Agur Lybeshari, Peter Makus, Lenny Mejía, Leon Merkel, Ardian Mile, Ylber Muceku, Dionald Muçollari, Naim Nazeri, Vilson Ndoni, Klei Prifti, Arben Radheshi, Indrit Rexhepi, Susann Richter, Gjon Rota, Zenel Rroko, Christoph Sens-Schönfelder, Gjergji Stoja, Marsel Tamo, Anila Xhahysa and Thomas Zieke.

References

Aliaj, Sh., J. Adams, S. Halchuk, E. Sulstarova et al. (2004). Probabilistic hazard maps for Albania, 13th WCEE Vancouver, Canada, August 1-6, 2469.

Aliaj, S., S. Kociu, B. Muço and E. Sulstarova (2010). Seismicity, Seismotectonics and Seismic Hazard Assessment in Albania, Academy of Sciences of Albania, 98.

Bulletin of the Albanian Seismic Network, Monthly bulletin of seismology, Albania, ISSN:2664-410X, https://www.geo.edu.al/Services/Department_of_Seismology/.

Custódio, S., N. A. Dias, B. Caldeira, F. Carrilho et al. (2014). Ambient noise recorded by a dense broadband seismic deployment in western Iberia, B. Seismol. Soc. Am., 104, 6, 2985-3007, doi:10.1785/0120140079.

Dushi, E. D. and J. Havskov (2023). 1D crustal structure of Albania region, Ann. Geophys., 66, 1, SE103, doi:10.4401/ag-8805.

Dushi, E., B. Rama, A. Schlömer, S. Egdorf et al. (2025). AdriaArray in Albania: Collaborative Deployment, station characterization and data integration, Ann. Gophys., submitted.

Ganas, A., P. Elias, P. Briole, F. Cannavo et al. (2020). Ground deformation and seismic fault model of the M6. 4 Durres (Albania) Nov. 26, 2019 earthquake, based on GNSS/INSAR observations, Geosci., 10, 6, 210, doi:10.3390/geosciences10060210.

Govorčin, M., S. Wdowinski, B. Matoš and G. J. Funning (2020). Geodetic source modeling of the 2019 Mw 6.3 Durrës, Albania, earthquake: Partial rupture of a blind reverse fault, Geophys. Res. Lett., 47, 22, e2020GL088990, doi:10.1029/2020GL088990.

Grad, M., T. Tiira and ESC Working Group (2009). The Moho depth map of the European Plate, Geophys. J. Int., 176, 1, 279-292, doi:10.1111/j.1365-246X.2008.03919.x.

Handy, M. R., J. Giese, S. M. Schmid, J. Pleuger et al. (2019). Coupled crust-mantle response to slab tearing, bending, and rollback along the Dinaride-Hellenide orogen, Tectonics, 38, 8, 2803-2828, doi:10.1029/2019TC005524.

Kolínský, P., T. Meier, M. R. Agius, AdriaArray Seismology Group et al. (2025). AdriaArray – a Passive Seismic Experiment to Study Structure, Geodynamics and Geohazards of the Adriatic Plate, Ann. Geophys., submitted.

Lindner, M., A. Rietbrock, L. Bie, S. Goes et al. (2023). Bayesian regional moment tensor from ocean bottom seismograms recorded in the Lesser Antilles: Implications for regional stress field, Geophys. J. Int., 233, 2, 1036-1054, doi:10.1093/gji/ggac494.

Lomax, A., J. Virieux, P. Volant and C. Berge-Thierry (2000). Probabilistic earthquake location in 3D and layered models: Introduction of a Metropolis-Gibbs method and comparison with linear locations, in C. H. Thurber and N. Rabinowitz (Eds.) Advances in Seismic Event Location, Modern Approaches in Geophysics, 18, Springer, Dordrecht, 101-134, doi:10.1007/978-94-015-9536-0_5.

Muço, B. (2013). Probabilistic seismic hazard assessment in Albania, Ital. J. Geosci., 132, 2, 194-202, doi:10.3301/ijg.2012.33.

NASA JPL (2013). NASA Shuttle Radar Topography Mission Global 1 arc second, Data set, NASA EOSDIS Land Processes Distributed Active Archive Center, doi:10.5067/MEaSUREs/SRTM/SRTMGL1.003.

Papadopoulos, G. A., A. Agalos, P. Carydis and E. Lekkas (2020). The 26 November 2019 Mw 6.4 Albania Destructive Earthquake, Seismol. Res. Lett., 91, 6, 3129-3138, doi:10.1785/0220200207.

Rossetti, F., M. G. Fellin, P. Ballato and C. Faccenna (2024). Building the Albanides by deep underplating, Tectonics, 43, 11, e2024TC008506, doi:10.1029/2024TC008506.

Schurr, B., E. Dushi, A. Rietbrock and L. Duni (2020). AlbACa Albanian Earthquake Aftershock Campaign, GFZ Data Services, Other/Seismic Network, doi:10.14470/4X7564679396.

Stipčević, J., M. Herak, I. Molinari and I. Dasović (2020). Crustal thickness beneath the Dinarides and surrounding areas from receiver functions, Tectonics, 39, 3, e2019TC005872, doi:10.1029/2019TC005872.

Styron, R. and M. Pagani (2020). The GEM Global Active Faults Database, Earthq. Spectra, 36, 160-180, doi:10.1177/8755293020944182.

Sulstarova, E. and Sh. Aliaj (2001). Seismic Hazard Assessment in Albania, Albania Journal of Natural and Technical Sciences, 10, 89-100.

Teloni, S., C. Invernizzi, S. Mazzoli, P. P. Pierantoni et al. (2021). Seismogenic fault system of the Mw 6.4 November 2019 Albania earthquake: New insights into the structural architecture and active tectonic setting of the outer Albanides, J. Geol. Soc. London, 178, 2, jgs2020-193, doi:10.1144/jgs2020-193.

Van der Heiden, V. (2021). Analysis of the 2019 Mw 6.4 Albania aftershock sequence: An updated velocity model using AI-based solutions, Master's thesis, Karlsruhe Institute of Technology, Geophysical Institute.

Vittori, E., A. M. Blumetti, V. Comerci, P. Di Manna et al. (2021). Geological effects and tectonic environment of the 26 November 2019, M w 6.4 Durres earthquake (Albania), Geophys. J. Int., 225, 2, 1174-1191, doi:10.1093/gji/ggaa582.

Wald, D. J. and T. I. Allen (2007). Topographic slope as a proxy for seismic site conditions and amplification, B. Seismol. Soc. Am., 97, 5, 1379-1395, doi:10.1785/0120060267.

Ward, K. M. and F. C. Lin (2017). On the viability of using autonomous three-component nodal geophones to calculate teleseismic Ps receiver functions with an application to Old Faithful, Yellowstone, Seismol. Res. Lett., 88, 5, 1268-1278, doi:10.1785/0220170051.

Woollam, J., A. Rietbrock, J. Leitloff and S. Hinz (2020). Hex: Hyperbolic event extractor, a seismic phase associator for highly active seismic regions, Seismol. Res. Lett., 91, 5, 2769-2778, doi:10.1785/0220200037.

Woollam, J., J. Münchmeyer, F. Tilmann and A. Rietbrock (2022). SeisBench-A toolbox for machine learning in seismology, Seismol. Res. Lett., 93, 3, 1695-1709, doi:10.1785/0220210324.

Yuan, X., J. Ni, R. Kind, J. Mechie et al. (1997). Lithospheric and upper mantle structure of southern Tibet from a seismological passive source experiment, J. Geophys. Res., 102, B12, 27491-27500, doi:10.1029/97JB02379.

Zhu, W. and G. C. Beroza (2019). PhaseNet: a deep-neural-network-based seismic arrival-time picking method, Geophys. J. Int., 216, 1, 261-273, doi:10.1093/gji/ggy423.

***CORRESPONDING AUTHOR: Hans AGURTO-DETZEL**,
Geophysical Institute, Karlsruhe Institute of Technology, Karlsruhe, Germany
e-mail: hans.detzel@kit.edu